Evidence for a Great Medieval Earthquake (~1100 A.D.) in the Central Himalayas, Nepal
Author(s): J. Lavé, D. Yule, S. Sapkota, K. Basant, C. Madden, M. Attal and R. Pandey
Source: *Science*, New Series, Vol. 307, No. 5713 (Feb. 25, 2005), pp. 1302-1305
Published by: American Association for the Advancement of Science
Stable URL: http://www.jstor.org/stable/3840223

the resonance frequency of the second qubit. The resulting drive current is off resonance with the second qubit; therefore, no appreciable coupling occurs for a time $\sim 0.1T_1$. In segment II, as the oscillations damp and come into resonance with the second qubit, the energy transferred to the second qubit is roughly quadratic in time and can be parameterized as $E_x/\hbar\omega_{10} \sim 10(C_x/C_j)^2[\omega_{10}(t_{delay} - 0.1T_1)]^2$. In segment III, as the measured qubit continues to decay and begins to sample the deepest harmonic regions of the right-hand well, the oscillation frequency moves above the resonance frequency of the second qubit. No additional energy is added, and the energy transferred to the second qubit levels out at a value $E_x/\hbar\omega_{10} \sim 100(C_x/C_j)^2\omega_{10}T_1$. Taking the probability for an $|0\rangle \rightarrow |1\rangle$ transition to be $P_1 \approx E_x/\hbar\omega_{10}$ for $E_x/\hbar\omega_{10} \ll 1$, we predict minimal measurement crosstalk for our circuit for $|t_{delay}| <$ 2 ns. Moreover, we note that the constraint on measurement timing becomes less stringent for qubits with longer T_1.

We investigated the dependence of measurement crosstalk on the timing of the measurements by repeating the experiment of Fig. 2 while varying t_{delay} to cover a total range of ±4 ns (Fig. 4C). When $t_{delay} > 2$ ns, the probability P_{11} is correlated with P_{10}; when $t_{delay} < 2$ ns, P_{11} is correlated with P_{01}. It is only when the relative delay of the measurements is optimally adjusted ($|t_{delay}| <$ 2 ns) that P_{11} is small and the oscillations in P_{11} disappear. Separate experiments indicate that when the timing of the measurement pulses is optimized, a tunneling event in one qubit results in a false measurement of $|1\rangle$ in the second qubit with only 15% probability. This residual measurement crosstalk can be attributed to the finite duration of the measurement pulse.

Our results suggest that it is possible in principle to perform high-fidelity measurements of multiple qubits. Such a technique may lead to scalable quantum information processing based on Josephson junctions.

References and Notes

1. M. A. Nielsen, I. L. Chuang, *Quantum Computation and Quantum Information* (Cambridge Univ. Press, Cambridge, 2000).
2. I. Chiorescu, Y. Nakamura, C. J. P. M. Harmans, J. E. Mooij, *Science* **299**, 1869 (2003); published online 13 February 2003 (10.1126/science.1081045).
3. J. M. Martinis, S. Nam, J. Aumentado, C. Urbina, *Phys. Rev. Lett.* **89**, 117901 (2002).
4. Yu. A. Pashkin *et al.*, *Nature* **421**, 823 (2003).
5. T. Yamamoto, Yu. A. Pashkin, O. Astafiev, Y. Nakamura, J. S. Tsai, *Nature* **425**, 941 (2003).
6. Y. Nakamura, Yu. A. Pashkin, J. S. Tsai, *Nature* **398**, 786 (1999).
7. D. Vion *et al.*, *Science* **296**, 886 (2002).
8. J. Kempe, K. B. Whaley, *Phys. Rev. A* **65**, 052330 (2002).
9. R. W. Simmonds, K. M. Lang, D. A. Hite, D. P. Pappas, J. M. Martinis, *Phys. Rev. Lett.* **93**, 077003 (2004).
10. K. B. Cooper *et al.*, *Phys. Rev. Lett.* **93**, 180401 (2004).
11. P. R. Johnson *et al.*, *Phys. Rev. B* **67**, 020509 (2003).
12. J. M. Martinis, M. H. Devoret, J. Clarke, *Phys. Rev. Lett.* **55**, 1543 (1985).
13. A. J. Berkley *et al.*, *Science* **300**, 1548 (2003); published online 15 May 2003 (10.1126/science.1084528).
14. At this frequency, the spectra of both qubits were free of fine structure normally attributed to spurious junction resonances (*9*).
15. R. McDermott *et al.*, data not shown.

16. Supported in part by the National Security Agency (NSA) Advanced Research and Development Activity (ARDA) through Army Research Office grants W911NF-04-1-2004 and MOD717304.

16 November 2004; accepted 6 January 2005
10.1126/science.1107572

Evidence for a Great Medieval Earthquake (~1100 A.D.) in the Central Himalayas, Nepal

J. Lavé,[1*†] D. Yule,[2*] S. Sapkota,[3] K. Basant,[3] C. Madden,[4] M. Attal,[1] R. Pandey[3]

The Himalayan orogen has produced three thrust earthquakes with moment magnitude (M_w) 7.8 to 8.5 during the past century, yet no surface ruptures associated with these great earthquakes have been documented. Here, we present paleoseismic evidence from east central Nepal that, since ~700 A.D., a single earthquake ruptured the Frontal Thrust fault at ~1100 A.D., with a surface displacement of ~17 (+5/−3) meters and a lateral extent and size that could have exceeded 240 kilometers and ~M_w 8.8, respectively. Ruptures associated with M_w <8.2 events would contribute to the frontal Himalayas folding but would stop before reaching the surface. These findings could require substantial modifications to current regional seismic hazard models.

The primary features of the Himalayan orogen are now understood, but the details of its seismotectonic behavior and maximum earthquake magnitudes are mostly unknown, despite their important implications regarding the seismic hazards facing densely populated regions. During the past century, the Himalayan arc has experienced three major thrust earthquakes of moment magnitude (M_w) >7.8. Growth folding (*1*, *2*) and surface faulting (*3*–*5*) have been reported in Holocene strata and terraces; paradoxically, none of these recent events reportedly produced coseismic surface ruptures, including the 1934 Bihar Nepal M_w 8.1 earthquake (*6*), which produced high-intensity shaking that was experienced throughout east Nepal and bordering regions of India (Fig. 1). To confirm the absence of rupture associated with this event and determine which events have led to the tectonic scarps, we conducted a paleoseismic study across the Himalayan front in the Marha Khola region, southeast of Kathmandu, in an area close to the inferred 1934 rupture zone.

Since ~20 million years ago, the deformation front resulting from the India/Asia collision has been expressed through the activation of two major thrust zones that are presumed to branch upward from a major midcrustal decollement: the Main Himalayan Thrust (*7*–*10*) (Fig. 1). In front of the rising Himalayas, thin-skinned thrust faulting has incorporated Cenozoic molasse deposits (Siwalik Formations) into the hanging walls of thrust faults, now expressed as the low-relief Siwalik Hills at the southern edge of the range. Geomorphic evidence of active tectonics indicates that 50 to 100% of the shortening across the Himalayas is transferred toward the southernmost of these faults, the Main Frontal Thrust fault (*2*, *5*, *11*). However, geodetic observations (*12*, *13*) indicate that current interseismic deformation is centered on a belt of microseismicity (*9*) that follows the southern edge of the Tibetan Plateau, ~100 km north of the frontal structure (Fig. 1). One explanation of this apparent paradox proposes that the current deformation mostly accumulates elastically at the transition along the decollement from steady creep beneath southern Tibet to locked beneath the High Himalaya, and that this elastic deformation releases and transfers to the front during large earthquakes (*2*, *9*), possibly like the 1934 M_w 8.1 earthquake.

[1]Laboratoire de Géodynamique des Chaînes Alpines, BP53, 38041 Grenoble, France. [2]California State University, Northridge, CA 91330, USA. [3]Seismolab, Department of Mines and Geology, Lainchaur, Kathmandu, Nepal. [4]Earth Consultants International, Tustin, CA 92780, USA.

*These authors contributed equally to this work.
†To whom correspondence should be addressed. E-mail: jlave@ujf-grenoble.fr

The study area at Marha Khola is well suited to test the above seismotectonic model: It is located west of the maximum intensity felt during this 1934 event (Fig. 1) but within the hypothetical 200- to 300-km-wide rupture segment (*14*) and also across the active Bagmati/Ratu anticline (fig. S1) (*15*), where numerous folded fluvial Holocene terraces indicate a full transfer of the convergence to the frontal structure (*2*). Along the Marha Khola, fluvial strath terraces (Fig. 2) have been uplifted 5 to 40 m above its present channel. A tectonic scarp marks the southern extent of these terraces (fig. S1) (*15*). The scarp is ~4 m high across the youngest uplifted terrace (HT_4) and exhibits a sinuous geometry (Fig. 2).

Trenches 1 and 2, excavated across this scarp, and trench 3, a riverbank exposure cleaned and extended to depth (Fig. 2), expose four stratigraphic units (Fig. 3). Unit 1, deposited above the HT_4 strath at ~700 A.D. (samples MA-4 or M-2-29), consists of a near-uniform, 3-m-thick sequence of fluvial gravel (Fig. 2B). Unit 2 overlies this sequence and varies laterally from a 20-cm-thick, organic-rich soil (trench 3) dated at 1000 to 1200 A.D. (samples M-3-5 and M-2-9) to >2.5 m of fine to coarse-grained fan material, with interlayered thin soil horizons (trench 1). Fluvial incision has truncated units 1 and 2 along a major unconformity, U_{2-3}. In trench 2, the unconformity is overlain in its western part by a sequence of fluvial gravels (unit 3) that bury the footwall and deposit a thin veneer on top of the frontal fold. Subsequently, unit 4 deposits (interlayered weak soil, slope wash, overbank, and fluvial materials capped by the present-day 40-cm-thick cultivated soil) were deposited between 1000 and 1900 A.D. (Fig. 4).

The tectonic scarp consists of several main fault zones (F1, F2, and F3) and related folds. All faults in trenches 1 and 2 and F3 in trench 3 have ruptured the fluvial sequence (units 1 and 2) and are sealed by units 3 and 4. The upper ruptures F1 and F2 in trench 3 break units 1 and 2, but no dateable constraint in the form of an intact overlying horizon exists (Fig. 3). According to the charcoal ages (Fig. 4 and table S1) (*15*), the faults ruptured the surface between 1020 and 1160 A.D. Although a complex scenario with two large ruptures spanning ~150 years could be envisaged, the simplest explanation of our observations, supported by a careful analysis of relationships in T2 (discussion S1) (*15*), is to conclude that faults F1, F2, and F3 are coeval and the timing of their rupture is constrained by the age of formation of the major U_{2-3} unconformity at ~1100 A.D. (Fig. 4).

Along the right bank of Marha Khola and northwest of the scarp, the HT_4 strath level and overlying unit 1 gravels exhibit a near-uniform uplift relative to the present Marha Khola floodplain (Fig. 2), consistent with a rigid-body translation above a thrust ramp at depth (*2*). Assuming an ~S20°W slip direction (Fig. 1) and uniform rigid-body uplift above a ~N70°W-striking 25° ± 5° dipping ramp (fig. S1) (*15*), the 7- to 7.5-m vertical separation of HT_4 would result from a slip event of 17 (+6/–4) m. In the trenches, a similar amount of slip, 17 (+5/–3) m, can be estimated from the strike and dip of the different fault segments and from the vertical separation, at some distance from the fault, of either the HT_4 strath level or the top of the fluvial sequence (unit 1) (table S2 and discussion S2) (*15*).

According to the classical view on scaling between slip value, rupture area, and magnitude (*16*), we would expect that the ~1100 A.D. earthquake ruptured a large segment of the Himalayan arc. Unfortunately, published scaling theories are inappropriate to estimate the extent and magnitude of large shallow thrust earthquakes (*16*). Consequently, the surface rupture observed at Marha Khola suggests two possible end-member hypotheses: a large earthquake ($7.6 \le M_w \le 8.1$) with slip enhancement close to the surface or a great earthquake ($8.4 \le M_w \le 8.8$) activating a large fault plane with an average rupture slip similar to the value observed at Marha Khola.

A possible analog to the first hypothesis, the recent M_w 7.6 Chi-Chi thrust earthquake (*17*, *18*) in the western foothills of Central Taiwan, locally produced surface slip of >10 m,

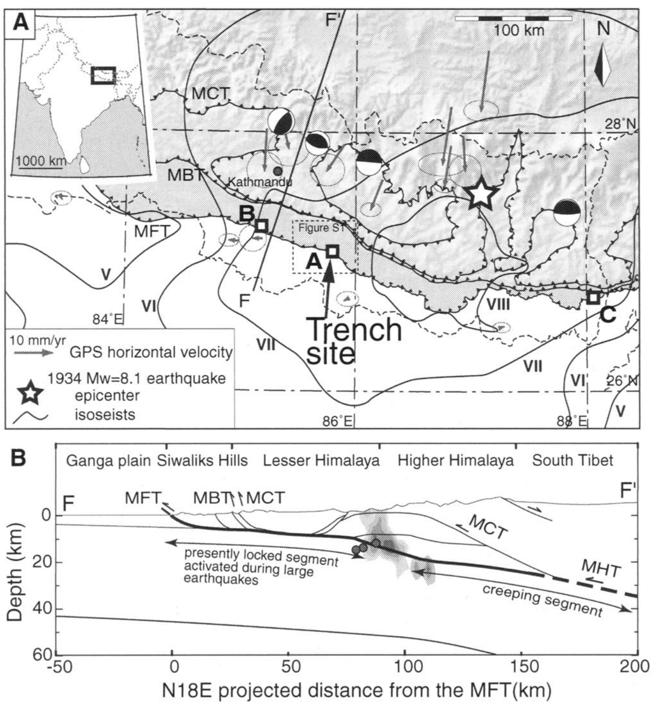

Fig. 1. (**A**) Map of eastern Nepal, including Global Positioning System (GPS) velocities relative to GPS stations in the Gangetic Plain (*23*), the focal mechanisms of the major earthquakes (M_w > 5) since 1965 [International Seismological Centre; Harvard solution (*24*)], and the epicenter of the M_w 8.1 1934 thrust earthquake (star) (*25*). The Marha Khola trench site (A) is located west of the most heavily shaken area (isoseismal MSK intensity contour = VIII) (*26*), ~240 km from a previous paleoseismic trenching study (C) in far east Nepal (*1*). At B, the Main Frontal Thrust fault slips at 21 ± 1.5 mm/year during the Holocene (*2*). (**B**) Simplified structural cross section across the central Himalayas of Nepal, with the major instrumental thrust earthquakes since 1965 (circles) and the cluster of microseismicity (*9*) (gray shading). MCT, Main Central Thrust; MBT, Main Boundary Thrust; MFT, Main Frontal Thrust; MHT, Main Himalayan Thrust.

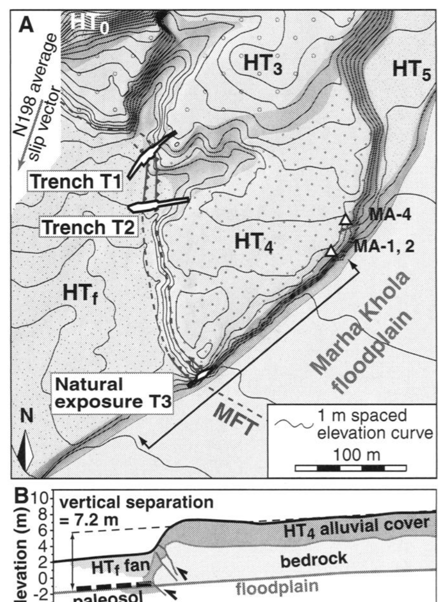

Fig. 2. (**A**) Topographic map of the trench site showing the location of trench exposures and the tectonic scarp of the Main Frontal Thrust fault (MFT) and uplifted terraces on the right bank of Marha Khola. (**B**) Cross section shows vertical separation across the fault of the top of HT_4 alluvial cover (vertical exaggeration = 5:1). Since scarp formation, active sedimentation (HT_f fan deposition) has occurred on the footwall to the southwest of the fault.

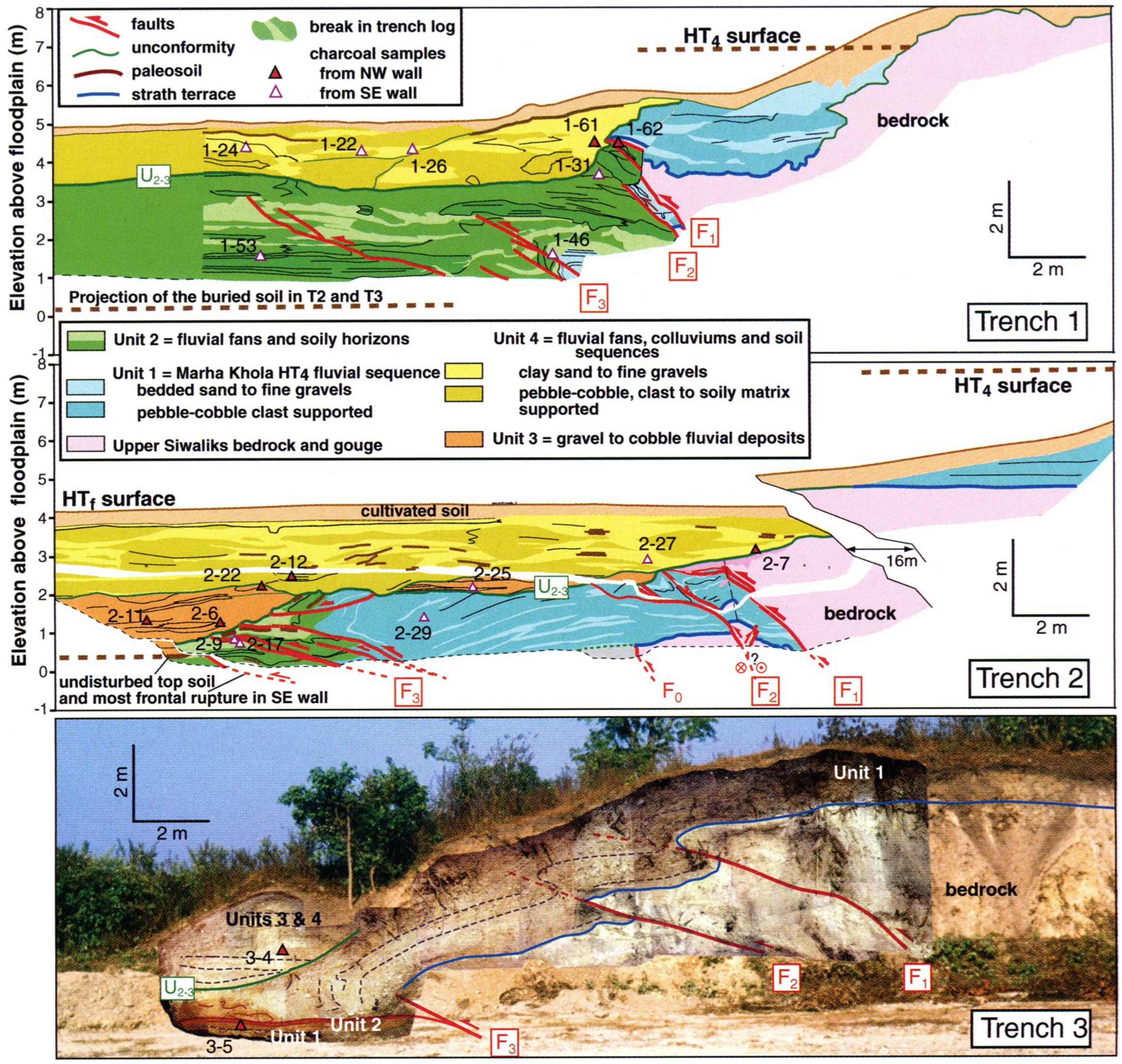

Fig. 3. Logs of the northwest walls of trenches 1 and 2 (**top**) and photograph of the northwest wall of trench 3 (**bottom**). Unconformity U_{2-3} (heavy green line) separates deformed from undeformed units, separating underlying pre-rupture from overlying post-rupture units, respectively. Triangles show locations of charcoal samples (see Fig. 4 for age data).

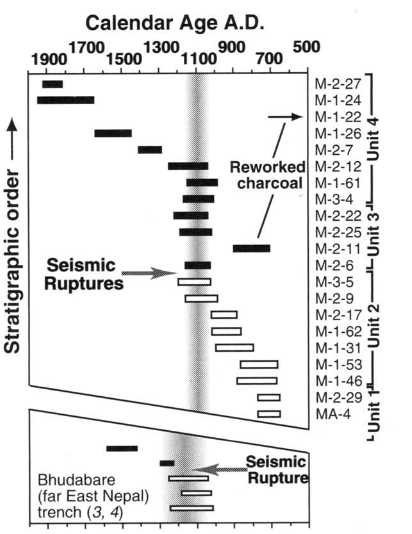

Fig. 4. Summary of the calendar radiocarbon ages, calibrated using CALIB 4.3 (*27*), from Marha Khola's trenches (table S1) (*15*) and from a trench in far East Nepal (*3*, *4*).

yet activated a relatively small rupture plane (30 × 80 km). Here, a Chi-Chi–type earthquake, of magnitude $M_w \leq 7.8$ (same rupture area but doubling slip), would release tectonic loading accumulated below the Siwaliks Hills or the southern part of the Lesser Himalayas.

A major conclusion of this study is the absence of surface rupture during the M_w 8.1 1934 Bihar Nepal earthquake, confirming previous reports (*3*, *14*). The rupture could have broken the vertical northern branch of the fault propagation fold (fig. S1) (*15*), but we did not observe a tectonic scarp across this northern fault, and subsidence in the Gangetic plain detected by leveling measurements (*19*) contradicts the hypothesis that the 1934 rupture propagated south of the Main Frontal Thrust fault (*7*). We suspect that earthquakes such as the 1934 event therefore could break the locked segment of the Main Himalayan Thrust (*2*, *12*) but die out before reaching the surface and deliver elastic strain at the southern tip of their rupture to active folding in the Siwalik Hills. This deformation, if elastically stored, could then be released during a Chi-Chi–type earthquake that activates the ramp and ruptures to the surface trace of the Main Frontal Thrust. Alternatively, a subsequent 1934-type event could activate the elastically stored energy and finally deliver slip to the surface, resulting in an unusually large surface displacement (maximized near the surface).

Two observations do not seem, however, to support these views. First, a summation of the seismic moment for the Himalayan arc reveals that the frequency of $M_w \cong 8.1$ earthquakes during the past three centuries is insufficient (*19*) to explain the transfer of most of the South Tibet/India convergence toward the frontal fold (*2*). Second, the absence of a surface rupture since the ~1100 A.D. event requires that elastic strain has been accumulating for ~830 years beneath the Siwaliks Hills. However, the uplift profiles of the youngest Holocene terraces across the Bagmati/Ratu anticline (fig. S1) (*15*) do not exhibit the expected component of elastic deformation (discussion S3 and fig. S2) (*15*). Rather, terrace profiles suggest that the ruptures associated with blind M_w <8.2 events contribute by permanent postseismic deformation to the long-term folding of the most frontal Himalayan structures.

In the second hypothesis, the large slip value observed at Marha Khola would have been produced by a great earthquake that ruptured a large segment of the Himalayan arc. In contrast with the M_w = 8.1 1934-type events, its seismic energy would have been sufficient for the rupture to propagate up to the surface. In this hypothesis, the ~1100 A.D. earthquake may have nucleated below the High Himalayas, as is suspected for the 1934 event, and broken through to the surface trace of the Main Frontal Thrust fault, a cross-strike distance of about 100 km (Fig. 1). Its lateral extent could have therefore reached or overcome the 200- to 300-km length that has been ascribed to the 1934 M_w 8.1 earthquake (*14*). A trench across the Main Frontal Thrust fault in far east Nepal (*3*, *4*) exposed a rupture with >4 to 8 m of slip that occurred between 1050 and 1300 A.D. (Fig. 4). If this surface rupture is synchronous to the ~1100 A.D. event, its lateral extent would reach at minimum 240 km. The magnitude of this earthquake would range from M_w 8.4 up to M_w 8.8 (*20*), assuming that the respective slip values observed in far east Nepal and Marha Khola trenches are representative of the average slip on the fault plane.

Additional paleoseismic studies are required to test the above hypotheses and to ascribe a more precise rupture length, mean slip, and magnitude to the inferred great medieval earthquake. For the moment, according to the worst scenario and to magnitude distribution law for thrust earthquakes in Nepal (*21*), the return period for a ~M_w 8.8 and 17-m mean slip event would range between 1800 and 3000 years at Marha Khola (with large uncertainties, given that the magnitude distribution law can not easily be extrapolated to large earthquakes). Such very large events would thus accommodate 25 to 50% of the shortening across the Himalayas, and if generalized to the whole Himalayan arc, would help to bring the seismic moment summation to closure (*19*). Between two such great earthquakes, the Main Himalayan Thrust can generate, in addition, several 7.5 < M_w < 8.2 events, but in the absence of surface ruptures, estimating the recurrence and slip for this type of Himalayan thrust earthquake is not possible using conventional paleoseismic trench studies.

References and Notes

1. T. Nakata, *Spec. Pap. Geol. Soc. Am.* **232**, 243 (1989).
2. J. Lavé, J. P. Avouac, *J. Geophys. Res.* **105**, 5735 (2000).
3. T. Nakata *et al.*, *Eos* **79**, F615 (1998).
4. B. N. Upreti *et al.*, Eds., *Proceedings of the Hokudan International Symposium and School on Active Faulting* (Letter Press, Hiroshima, Japan, 2000), pp. 533–536.
5. S. Kumar *et al.*, *Science* **294**, 2328 (2001).
6. N. N. Ambraseys, J. Douglas, *Geophys. J. Int.* **159**, 165 (2004).
7. L. Seeber, J. Armbuster, Eds., *Earthquake Prediction: An International Review* (Maurice Ewing Series, American Geophysical Union, Washington, DC, 1981), pp. 259–277.
8. W. Zhao, K. D. Nelson, Project INDEPTH Team, *Nature* **366**, 557 (1993).
9. M. R. Pandey, R. P. Tandukar, J. P. Avouac, J. Lavé, J. P. Massot, *Geophys. Res. Lett.* **22**, 751 (1995).
10. J. Lavé, J. P. Avouac, *J. Geophys. Res.* **106**, 26,561 (2001).
11. S. G. Wesnousky, S. Kumar, R. Mohindra, V. C. Thakur, *Tectonics* **18**, 967 (1999).
12. M. Jackson, R. Bilham, *J. Geophys. Res.* **99**, 13897 (1994).
13. R. Bilham, K. Larson, J. Freymuller, Project Idylhim Members, *Nature* **386**, 61 (1997).
14. M. R. Pandey, P. Molnar, *J. Geol. Soc. Nepal* **5**, 22 (1988).
15. Supporting material is available on *Science* Online.
16. C. H. Scholz, *The Mechanics of Earthquakes and Faulting* (Cambridge Univ. Press, Cambridge, ed. 2, 2002), pp. 179–243.
17. H. F. Ma, *Eos* **80**, 605 (1999).
18. S. Dominguez, J. P. Avouac, R. Michel, *J. Geophys. Res.* **108**, 2083 (2003).
19. R. Bilham, V. Gaur, P. Molnar, *Science* **293**, 1442 (2001).
20. M_w was computed from Kanamori's relation (*22*) for the seismic moment $M_w = 2/3\log_{10}(M_0) - 6$, where $M_0 = \mu \times \text{slip} \times L \times W$ (where L and W are the rupture length and width), the shear modulus $\mu = 3.3 \times 10^{10}$ N/m², W = 100 km from the locking zone below the High Himalayas to the Main Frontal Thrust fault, $L \geq 240$ km, and the average slip equals 5 to 17 m.
21. J. P. Avouac, L. Bollinger, J. Lavé, R. Cattin, M. Flouzat, *C. R. Acad. Sci.* **333**, 513 (2001).
22. H. Kanamori, *Tectonophysics* **93**, 185 (1983).
23. K. Larson, R. Bürgmann, R. Bilham, J. Freymueller, *J. Geophys. Res.* **104**, 1077 (1999).
24. P. Molnar, *J. Him. Geol.* **1**, 131 (1990).
25. W. P. Chen, P. Molnar, *J. Geophys. Res.* **82**, 2945 (1977).
26. N. N. Ambraseys, J. Jackson, *Curr. Sci.* **84**, 570 (2003).
27. M. Stuiver, P. J. Reimer, *Radiocarbon* **35**, 215 (1993).

28. This research was supported by the French program Programme National de Recherche sur les Risques Naturels. We are most grateful to the National Seismological Center, Kathmandu, and the Laboratoire de Détection Géophysique for their logistic help in the organization of the field surveys. A. Gajurel kindly provided help logging the trenches. We are indebted to G. Seitz for analyzing some of the charcoal samples at the Center for Accelerator Mass Spectrometry, Lawrence Livermore National Laboratory, California. We thank J. P. Avouac, K. Sieh, and two anonymous reviewers for insightful comments on earlier drafts of the manuscript.

Supporting Online Material

www.sciencemag.org/cgi/content/full/307/5713/1302/DC1

SOM Text

Figs. S1 and S2

Tables S1 and S2

References

2 September 2004; accepted 18 January 2005

10.1126/science.1104804

How Science Survived: Medieval Manuscripts' "Demography" and Classic Texts' Extinction

John L. Cisne

Determining what fraction of texts and manuscripts have survived from Antiquity and the Middle Ages has been highly problematic. Analyzing the transmission of texts as the "paleodemography" of their manuscripts yields definite and surprisingly high estimates. Parchment copies of the foremost medieval textbooks on arithmetical and calendrical calculation closely fit age distributions expected for populations with logistic growth and manuscripts with exponential survivorship. The estimated half-lives of copies agree with Bischoff's paleographically based suggestion that roughly one in seven manuscripts survive in some form from ninth-century Carolingian workshops. On this basis, many if not most of the leading technical titles circulating in Latin probably survived, even from late Antiquity.

Every student learns that the germ of his or her science barely made it through the Middle Ages. Just how likely were individual handwritten books to survive, or entire works to be lost? So far, the best evidence has come from the histories of individual manuscripts, libraries, and texts as reconstructed by paleographers, and it is overwhelmingly anecdotal.

Because manuscripts, unlike printed material, must be copied individually from antecedents, like organisms, their multiplication likewise should be inherently exponential. By treating the manuscripts of a

Department of Earth and Atmospheric Sciences, Cornell University, Ithaca, NY 14853, USA. E-mail: cisne@geology.cornell.edu